Contents lists available at ScienceDirect

Psychiatry Research: Neuroimaging

Test-retest reliability of resting-state cerebral blood flow quantification using pulsed Arterial Spin Labeling (PASL) over 3 weeks vs 8 weeks in healthy controls

Alexandra Kyrou [a,b,^], Elina Grünert [a,b,^], Florian Wüthrich [a,b], Niluja Nadesalingam [a,b], Victoria Chapellier [a,b], Melanie G Nuoffer [a,b,c], Anastasia Pavlidou [a,b], Stephanie Lefebvre [a,b,*,#], Sebastian Walther [a,b,#]

[a] University Hospital of Psychiatry and Psychotherapy Bern, Translational Research Center, University of Bern, Switzerland
[b] Translational Imaging Center (TIC), Swiss Institute for Translational and Entrepreneurial Medicine, Bern, Bern, Switzerland
[c] Graduate School for Health Sciences, University of Bern, Bern, Switzerland

ARTICLE INFO

ABSTRACT

Arterial Spin Labeling is a valuable functional imaging tool for both clinical and research purposes. However, little is known about the test-retest reliability of cerebral blood flow measurements over longer periods. In this study, we investigated the reliability of pulsed Arterial Spin Labeling in assessing cerebral blood flow over a 3 (n = 28) vs 8 (n = 19) weeks interscan interval in 47 healthy participants. As a measure of cerebral blood flow reliability, we calculated voxel-wise, whole-brain, and regions of interest intraclass correlation coefficients. The whole-brain mean resting-state cerebral blood flow showed good to excellent reliability over time for both periods (intraclass correlation coefficients = 0.85 for the 3-week delay, intraclass correlation coefficients = 0.53 for the 8-week delay). However, the voxel-wise and regions of interest intraclass correlation coefficients fluctuated at 8-week compared to the 3-week interval, especially within cortical areas. These results confirmed previous findings that Arterial Spin Labeling could be used as a reliable method to assess brain perfusion. However, as the reliability seemed to decrease over time, caution is warranted when performing correlations with other variables, especially in clinical populations.

1. Introduction

Arterial Spin Labeling (ASL) is a non-ionizing magnetic resonance imaging (MRI) technique that uses magnetically labeled arterial blood water as a tracer to quantify cerebral blood flow (CBF) (Alsop et al., 2015). A rise in CBF occurs in a precise spatial and temporal manner to provide an adequate oxygen supply to working neurons (Buxton and Frank, 1997; Golay et al., 2004; Grade et al., 2015). Even if CBF is not a direct measure of neural activity, it is a closely coupled correlate (Borogovac and Asllani, 2012). ASL consists of a differential technique during which two acquisitions are carried out: one with the labeling of arterial protons and one without labeling which serves as control acquisition. Different ASL acquisition methods can be used to

magnetically label arterial blood water: including continuous ASL (cASL), pseudocontinous ASL (pcASL), and pulsed ASL (PASL), depending on the frequency and amount of radiofrequency (magnetic) pulses applied (continuous/ ray of pulses/singular pulse) (Alsop et al., 2015). These methods differ regarding the signal-to-noise ratio and the image resolution. PASL has been developed to overcome the caveats of the cASL technique, and pcASL offers a better signal-to-noise ratio than the two other methods (Alsaedi et al., 2018). The clinical applications of ASL acquisition in assessing brain perfusion as a diagnostic tool, are manifold, with the main focus on vascular diseases, such as stroke and arteriovenous malformations and neurodegenerative diseases, mainly in Parkinson`s, Alzheimer`s disease, and other types of dementia (Alsop et al., 2015; Claassen et al., 2021; Haller et al., 2016; Hernandez-Garcia

et al., 2019; Ho, 2018). However, in order to use resting-state CBF (rs-CBF) as measured by ASL as a biomarker of a condition or an outcome marker of treatment effects, the measure needs to be highly reliable. Currently, the rs-CBF fluctuations over time are largely unknown. Quantifying the range of normal fluctuation is needed.

Reliability of brain signals can be measured using different metrics. In functional neuroimaging, one crude way to evaluate the consistency of brain activation relies on the comparison of the amplitude and spatial extent of the activated areas between time points on a group level. This easy method fails to evaluate intra-individual variability. Reliability could also be assessed through the within-subject coefficient of variation (wsCV), which is typically calculated with the ratio of the standard deviation of the difference between repeated measurements to the mean of repeated measurements (Bland and Altman, 1996). For example, Bland-Altman plots could be used to evaluate agreements between two measurements. Finally, intraclass correlation coefficients (ICC) can assess the amplitudes or weights of activations within voxels or regions of interest (ROIs) over time and have become a standard method to evaluate reliability over time (Giraudeau et al., 2000; Shrout and Fleiss, 1979).

Previous studies on rs-CBF measurements yielded conflicting results in predominantly small samples. Most studies exploring short-term changes of less than 1 week suggested overall good reliability for both whole-brain and regions of interest (ROIs) rs-CBF quantification. In 31 participants, Almeida et al. showed good reliability (ICC ranging from 0.42 to 0.81) of the rs-CBF for most of the ROIs over one week(Almeida et al., 2018). Chen et al. (Chen et al., 2011) compared the mean whole-brain rs-CBF quantification acquired with different labelling methods (PASL, cASL and pcASL) over one hour and one week in 12 healthy controls. The three methods showed overall good reproducibility, as measured with ICC over time (ICC > 0.65). However, reproducibility as measured with the within-subject coefficient of variation seemed to decrease slightly over time, indicating physiological fluctuations. The studies exploring reliability with longer interscan interval showed more variability with the degree of the reliability depending on the brain areas. Gevers et al. evaluated the reliability of rs-CBF quantification with the three ASL acquisition methods between either different scanners or over a 3-weeks period in 6 healthy controls. Mean whole-brain rs-CBF showed fair reliability over time with the three ASL methods using the coefficient of repeatability and the repeatability index as reliability measure(Gevers et al., 2011). Mezue et al. used a pcASL protocol to assess region of interest (ROIs) rs- and task-based CBF in 8 healthy participants over periods of 30 min (within-session), 1-week and 1-month. Although within-session and 1-week period showed an overall fair to excellent reliability of the rs-CBF ($0.40 < ICC < 0.93$), after one month the reliability varied from poor to good depending on the ROIs demonstrating substantial heterogeneity in the long-term reliability of rs-CBF ($0.06 < ICC < 0.589$)(Mezue et al., 2014). Using the same time scale, Ssali et al. observed fair to excellent reliability ($0.44 < ICC < 0.94$) of the mean whole-brain, voxel-wise, and ROIs rs-CBF over time in 7 healthy participants(Ssali et al., 2016). Jiang et al. examined the reliability of whole-brain, and ROIs rs-CBF measured with PASL in 12 cognitively normal elderly subjects (60–80 years old) over 3, 6 and 12 months. The excellent reliability and reproducibility observed after 3 months ($ICC > 0.97$), decreased slightly to moderate after one year ($0.63 < ICC < 0.74$) (Jiang et al., 2010). Finally, a recent multi-center study showed highly variable reliability depending on the brain area ($0.00 < ICC < 0.70$) of the rs-CBF in some regions of the Default Mode Network in 10 participants, with the between-scans interval ranging from 2 to 218 days(Ibinson et al., 2022).

Collectively, while rs-CBF reliability is excellent up to one week in healthy participants, the reliability of the rs-CBF over longer interscan intervals requires further study. Moreover, only a single small ($n = 7$) study(Ssali et al., 2016) performed a voxel-wise reliability analysis, which might have a greater clinical relevance as affected regions by the pathology or the symptoms may not be known a priori.

Accordingly, the current study aimed to provide an up-to-date reliability evaluation of the rs-CBF quantification provided by PASL using two moderately large samples of healthy young adults. To address this topic, we investigated i) voxel-wise rs–CBF reliability, ii) whole-brain rs-CBF reliability, and iii) rs-CBF reliability in ROIs over two longer interscan intervals (3 and 8 weeks) in healthy, young participants. We expected overall stable rs-CBF parameters for both interscan intervals, but a slight drop in reliability for the 8-weeks interscan interval especially in the ROIs analysis.

2. Material and methods

2.1. Population

We performed a sample size estimation for hypothesis-driven ICC calculation (Walter et al., 1998). As hypothesized, in a 3-week delay, the whole-brain level CBF calculation was expected to reach good to excellent reliability. Thus, the following parameters were used for the estimation: expected reliability = 0.75, minimum acceptable reliability = 0.4, expected drop out for image quality and motion = 20 % (Fallatah et al., 2018), significance level = two-tailed 0.05, power= 0.80, number or raters/repetition per subject = 2; and led to a minimum sample size of $n = 35$. Accordingly, we recruited healthy participants from the general population in Switzerland as controls for two clinical trials [$n = 42$ for OCoPS-P (Overcoming Psychomotor Slowing in Psychosis) ClinicalTrials.gov Identifier: NCT03921450 (Walther et al., 2024); and $n = 35$ for BrAGG-SoS (Chapellier et al., 2022) (The Brain Stimulation And Group Therapy to Improve Gesture and Social Skills in Psychosis trial, NCT04106427)]. Participants were recruited via advertisements and word of mouth. Inclusion criteria were right-handedness assessed by the Edinburgh Handedness Inventory (Oldfield, 1971), age between 18 and 60 years, and ability/willingness to participate in the study. Exclusion criteria were substance abuse other than nicotine, history of psychiatric disorders or medical conditions impairing movements (assessed by the MINI international neuropsychiatric interview), epilepsy, history of head trauma with loss of consciousness, and MRI contraindications (assessed by an MRI safety questionnaire), that is, metal objects in the body or pregnancy (assessed by a pregnancy test). All participants provided written informed consent. The study protocols adhered to the Declaration of Helsinki and were approved by the local ethics committee. We split these participants into two samples to explore the longitudinal reliability of CBF measures based on the clinical trial protocols. The first one (Sample-3 W), $n = 42$, was used for reliability analysis of the 3-week interscan interval, and the second one (Sample-8 W), $n = 35$, for the 8-week interscan interval. In the Sample-3 W, 28 out of 42 participants were included in the analyses while in the Sample-8 W, 19 out of 35 participants were included in the analyses. Reasons for data exclusion were cancellation of the second session (Sample-3 W $n = 5$, Sample-8 W $n = 8$), excessive motion in the scanner, or poor functional MRI data quality in at least one of the two sessions (Sample-3 W $n = 9$, Sample-8 W $n = 8$).

2.2. MRI acquisition and preprocessing

Participants underwent two imaging sessions that were scheduled three (Sample-3 W) or eight weeks (Sample-8 W) apart at the same weekday and approximately at the same hour of the day for both sessions. For each MRI session, we acquired a 3-D T1 MP2RAGE and a PASL sequence at the translational imaging center of the Swiss Institute for Translational and Entrepreneurial Medicine, Bern, Switzerland. The MRI scans were acquired on a 3 T Prisma MRI whole-body scanner using a 20-channel radio-frequency head coil (Siemens, Germany). Participants lay horizontally in the MR scanner with arms beside the trunk, we instructed them to avoid head motion and stay awake without specific instructions on keeping eyes open or closed.

2.2.1. Acquisition

The MRI protocol included the following 3 sequences:

1. 3D-T1-weighted MP2RAGE images (8 min 22 s covering 176 sagittal slices, 1 mm thick, TR = 5000 ms, TE = 2.98 ms, FOV=240 × 256 mm, flip angle 1= 4°, flip angle 2= 5°, voxel size = 1 × 1 × 1 mm).

2. A Perfusion MRI scan with T2* weighted images using a PASL sequence: TR= 3300 ms, TE =13 ms; flip angle = 90°; field of view (FOV) = 230 × 230 mm, 22 slices; thickness = 6 mm; no gap; number of dynamics = 90 (45 pairs of unlabeled and labeled images); bolus duration = 700 ms, inversion time (post-labeling delay) = 2200 ms, acquisition duration = 5.05 min, Voxel size = 3.6 × 3.6 × 6 mm.

3. A field map scan for use in unwarping EPI distortions due to magnetic field inhomogeneity: FOV = 230 × 230 mm, 22 slices; thickness = 6 mm, TR = 520 ms, TE1 = 4,92 ms, TE2 = 7.38 ms, Flip angle = 60°, thickness = 6 mm, Voxel size = 3.6 × 3.6 × 6 mm, acquisition duration = 2.13 min.

2.2.2. MRI preprocessing

We performed the MRI data preprocessing using SPM12 (Revision 7771, Welcome Trust, London, UK, https://www.fil.ion.ucl.ac.uk/spm/) and MATLAB (R2020b, MathWorks, Natick, USA). The preprocessing was identical for both sessions in both samples. After realigning and unwrapping the PASL sequence to correct for head motion and distortion due to field inhomogeneity, we quantified rs-CBF (ml/100 g/min) according to a previously applied, standardized protocol (Maderthaner et al., 2023)'(Muller et al., 2021). Rs-CBF maps were co-registered to the corresponding raw T1–3D. Raw T1–3D scans were then segmented and normalized to MNI space using the CAT12 (CAT12.8.2 (2130)) toolbox (http://www.neuro.uni-jena.de/cat/). The obtained deformation matrix was used to normalize the co-registered rs-CBF maps. We applied a 6 mm FWHM kernel to the normalized images. This standard preprocessing procedure was followed by a denoising step using subject-wise first-level generalized linear models with the white matter (WM) and cerebrospinal fluid (CSF) signal and the 6 motion parameters from realignment as explanatory variables (Maderthaner et al., 2023,Muller, 2021 #21) .We used the normalized mean rs-CBF maps for further analysis. For quality control, we checked six motion parameters (x-, y-, z-translations, roll, pitch, and yaw) and set a limit of 2.5 mm in one of the three translations or 2.5° in one of the three rotations for exclusion.

2.2.3. Regions of interest

We performed ROI-based analysis by extracting the mean rs-CBF values from the mask of each cortical and subcortical ROI of the Harvard-Oxford atlas (Desikan et al., 2006; Frazier et al., 2005; Goldstein et al., 2007; Makris et al., 2006), as well as the tissue type segmentation (grey matter, white matter, and CSF), and the cerebellum from the MNI structural atlas.

2.3. Statistics

To assess the reliability of rs-CBF measures in this test-retest study, we performed an intraclass correlation coefficient (ICC) analysis. ICC estimates and their 95 % confidence intervals were calculated using IBM SPSS Statistics Program (Version: 28.0.0.0 (190). SPSS Inc, Chicago, IL) based on a mean-rating (k = 2; i.e., the two specific sessions), absolute-agreement (as we aimed to evaluate the intra-individual reliability), 2-way mixed-effects model (ICC $_{(3,k)}$)(Koo and Li, 2016) between the two sessions in each sample (Sample-3 W and Sample-8 W). ICC $_{(3,k)}$ (hereafter ICC) is

ICC $(3, k) = \frac{BMS - EMS}{BMS + \frac{BMM - EMS}{n}}$ where BMS is the between-subject mean square, EMS is the error mean square, and BMM is the between-measurement mean square. ICC analysis has become a standard for several types of reliability analyses and ranges from 0 to 1. For interpretation, we applied the guidelines of Cicchetti(Cicchetti, 1994);

Coefficients below 0.4 will be considered poor; between 0.4 and 0.59, fair; between 0.6 and 0.74, good and >0.75, excellent. We performed a power calculation for each measured ICC using the ICC.Sample.Size (version 1.0) package in R (version 4.3.1); with the following formula: calculateIccPower(ICCobserved,ICCestimated,k,alpha,tails,N) where ICC rsobserved corresponds to the measured ICC, ICCestimated corresponds to 0.60 for the 3-week delay (at least good reliability) and 0.4 for the 8-week delay (at least fair reliability), k corresponds to 2 (the two sessions), alpha= 0.05, tails=2 and $N = 28$ for the 3-week delay and 19 for the 8-week delay.

2.3.1. Group comparisons

The comparison of the two samples in terms of demographics or baseline rs-CBF was performed in order to test for confounding information that could explain potential difference in terms of reliability.

Using SPSS, we compared the two samples for age using an independent two-sample *t*-test and sex distribution using a chi-square test.

To compare samples at baseline, we performed *t*-tests between the two samples for whole-brain mean rs-CBF, the whole-brain and the ROIs mean rs-CBF maps of the first scan session.

2.3.2. Reliability analysis

We first modelled paired *t*-tests between sessions to evaluate whether there were significant differences in the whole brain rs-CBF between the two sessions within each sample using two different thresholds: a strict voxel level correction for multiple comparison of $p_{FWE}<0.05$, and a less stringent one using a cluster forming threshold of $p_{uncorr}<0.001$ as well as a cluster correction for multiple comparisons of qFDR<0.05. Then, we performed a voxel-wise ICC analysis by calculating the absolute agreement ICC of each voxel of the brain mask (excluding CSF) using a homemade script in MATLAB. Then, we performed an ICC analysis on the whole-brain mean rs-CBF quantification and we calculated the Bland-Altman plots to demonstrate the reproducibility. Finally, we used the ROIs extracted mean rs-CBF values to perform ROI-based ICC analyses with SPSS, in each of the two samples.

3. Results

3.1. Comparison between the two samples at baseline

3.1.1. Demographics and behavioral comparisons

Participants of the Sample-3 W were significantly younger ($p = 0.043$) whereas the two groups were comparable in terms of sex distribution ($p = 0.9$). Participants in both samples had at least a good level of social functioning as defined by Global Assessment of Functioning (GAF) (Endicott et al., 1976) score >81 points, with the Sample-8 W presenting a slightly superior functioning ($p = 0.013$) (Table 1).

3.1.2. Mean rs-CBF

T-test of the whole-brain mean rs-CBF maps using age and sex as covariates, showed no significant differences between baseline sessions of the two samples (voxel level, $p_{FWE} <0.05$). While using a less stringent

Table 1
Demographics of the two samples.

	Sample-3 W (n = 28)	Sample-8 W (n = 19)	Statistics
Age (years) Mean ± SD	33.9 ± 11.1	40.9 ± 11.7	t(45)=−2.087, p = 0.043 *
Women (n,%)	16 (57.1 %)	11 (57.9 %)	X^2 (df=1, N = 47)= 0.003, p = 0.959
GAF score Mean ± SD	89.3 ± 7.2	95.6 ± 9.5	t (45)=−2.574, p = 0.013 *

GAF: Global Assessment of Functioning; SD: standard deviation; Sample-3W: sample for the 3-week interscan interval; Sample-8W: sample for the 8-week interscan interval.

threshold (cluster forming threshold $p_{uncorr}<0.001$, cluster corrected qFDR<0.05), Sample-3 W demonstrated slightly higher rs-CBF within bilateral thalamus, right putamen and right insula (Table 2, Fig. 1).We found no significant differences at baseline between the mean rs-CBF extracted in whole-brain, grey matter, white matter, and the cortical and subcortical ROIs of the two samples (Table 3).

3.2. Reliability analyses

3.2.1. Whole brain paired t-test comparison

Paired *t*-tests of the whole-brain mean rs-CBF maps showed no significant differences between the two sessions in the two samples.

3.2.2. Voxel-wise ICC

The ICC maps displayed in Fig. 2, show that the Sample-3 W had more widespread cortical brain regions with fair to excellent reliability (ICC > 0.4) between-sessions compared to the Sample-8 W. The reliability metrics within the cerebellum and subcortical regions seemed to be consistent between the two samples.

3.2.3. ROIs ICC

Table 4 gives the ICCs and corresponding statistical power. The ICCs of the extracted mean rs-CBF demonstrated excellent reliability (ICC >0.80) for the whole brain, grey matter, and white matter for the 3-weeks interscan interval, while reliability massively decreased for the 8-weeks interval (0.25 < ICC <0.56) (it remains at a fair level for the whole brain ICC = 0.53), especially in the left grey matter (ICC = 0.25) (Table 4, part A, Fig. 3).

The ROIs derived from brain parcellation demonstrated various levels of reliability for the two samples (Table 4, part B). On average, the 3-weeks interscan interval presented a better mean rs-CBF reliability, especially for cortical regions. More than 30 cortical regions showed at least fair reliability (ICC > 0.4) in the Sample-3 W and poor reliability (ICC < 0.38) in the Sample-8 W. The mean rs-CBF of the cerebellum seems to be reliable at both intervals (Sample-3 W (ICC = 0.85), Sample-8 W (ICC = 0.761)) while subcortical grey matter structures presented a variable level of reliability with some structures showing stronger reliability for the 8-weeks interscan interval. Seven subcortical regions had poor reliability in the Sample-3 W (ICC < 0.39) and at least fair reliability in the Sample-8 W (ICC > 0.41).

4. Discussion

Up to now, this is the largest study to evaluate rs-CBF reliability in healthy participants as measured by ICC at one and two months, using three different reliability evaluation levels; i) whole brain comparison between the two sessions, ii) voxel-wise reliability, iii) region of interest analyses including regions consisting of the whole brain as well as a full brain coverage by a standard parcellation (Harvard-Oxford Atlas). In line with our hypotheses, we demonstrated that within a month the

Table 2
Whole-brain rs-CBF maps comparison at baseline between the two samples (Cluster forming threshold puncorr<0.001, cluster corrected qFDR<0.05).

	Cluster corrected p (FDR-corr)	Cluster size	x	y	z	Brain Area
Sample-3 *W* > Sample-8W	0.048	293	−14	−22	18	Bilateral thalamus
	0.046	469	34	−28	20	Right putamen/ Right insula

p FDR-corr: p value corrected at False discovery rate; Sample-3W: sample for the 3-week interscan interval; Sample-8W: sample for the 8-week interscan interval.
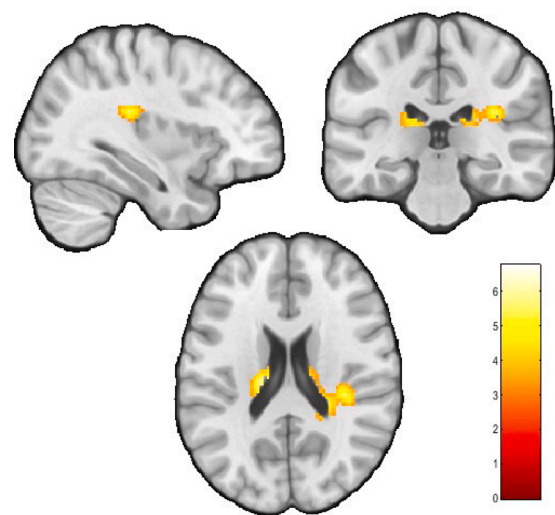

Fig. 1. Whole-brain rs-CBF maps comparison at baseline between the two samples. Cluster forming threshold $p_{uncorr}<0.001$, cluster corrected qFDR=0.046. Displayed are the brain areas showing higher rs-CBF levels at baseline in the Sample-3 W compared to the Sample-8 W.
Sample-3W: sample for the 3-week interscan interval; Sample-8W: sample for the 8-week interscan interval; rs-CBF: resting-state cerebral blood flow; qFDR: p value corrected at False discovery rate; p_{uncorr}: uncorrected p value.

Table 3
Baseline comparison of the mean rs-CBF in the whole brain, different tissue types, and selected ROIs. (Cluster forming threshold $p_{uncorr}<0.001$, cluster corrected qFDR).

Brain parcellation	rs-CBF Mean ± SD (ml/100 g/min) Sample-3W	rs-CBF Mean ± SD (ml/100 g/min) Sample-8W	Statistics
Whole Brain	33.2 ± 7.2	35.3 ± 5.9	t (45)=− 0.0327, p = 0.745
Left grey matter	33.4 ± 6.9	34.9 ± 5.4	t (45)=−0.822, p = 0.415
Left white matter	32 ± 6.6	33.5 ± 6.6	t (45)=−0.817, p = 0.418
Right grey matter	34.3 ± 7.4	34.7 ± 5.6	t (45)=−0.156, p = 0.876
Right white matter	35.3 ± 7.2	35.9 ± 5.4	t (45)=−0.092, p = 0.927
Frontal medial cortex	29 ± 9.2	34.2 ± 7	t (47)=−1.854, p = 0.070
Left hippocampus	29.0 ± 9.5	34.2 ± 9.2	t (47)=0.873, p = 0.387
Left putamen	31.8 ± 6.7	22.5 ± 9.8	t (47)=−0.568, p = 0.573
Parietal operculum cortex	22.5 ± 9.4	23.8 ± 8.5	t (47)=0.596, p = 0.554
Postcentral gyrus	27.9 ± 6.4	26.3 ± 5.8	t (47)=−1.549, p = 0.128
Precentral gyrus	27.0 ± 7.2	29.9 ± 5.7	t (47)=−1.614, p = 0.113
Right thalamus	26.8 ± 10.8	29.9 ± 12.7	t (47)=0.543, p = 0.589
Temporal pole	32.8 ± 6.9	29.8 ± 6.4	t (47)=−0.587, p = 0.560

SD: standard deviation;rs-CBF: resting-state cerebral blood flow; Sample-3W: sample for the 3-week interscan interval; Sample-8W: sample for the 8-week interscan interval.

voxel-wise, whole brain and region of interest rs-CBF quantification showed overall good to excellent reliability. The rs-CBF reliability slightly decreased after two months, especially in cortical areas. The different methods provided convergent results.
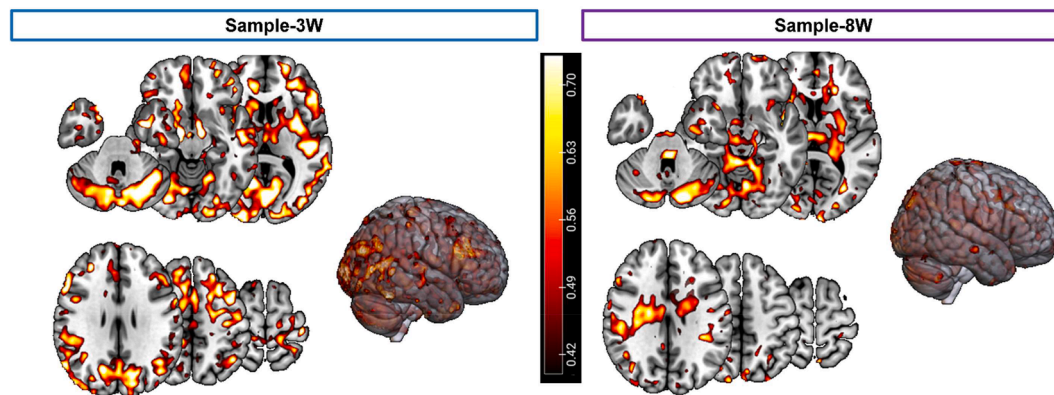
Fig. 2. Voxel-wise ICC. This figure displays for each sample the brain areas showing at least fair reliability (ICC > 0.4). The central bar refers to the intensity of the ICC. *Sample-3W: sample for the 3-week interscan interval; Sample-8W: sample for the 8-week interscan interval; p value. ICC: intraclass correlation coefficient.*

When assessed with a 3-week interscan interval, the rs-CBF at the whole brain level seems highly reliable (with an excellent reliability estimation, ICC = 0.85; power = 0.82). The voxels-wise reliability confirms this observation showing that overall voxels within most cortical and subcortical regions including the cerebellum showed good to excellent reliability. Particularly high reliability of rs-CBF was found in the ROIs of motor and premotor regions, prefrontal, parietal and visual cortices as well as amygdala, caudate, and putamen. The signal reliability assessed by ICC decreases slightly between 3 and 8 weeks at the whole brain level from ICC = 0.85 to ICC = 0.53. This confirms previous findings(Almeida et al., 2018; Chen et al., 2011; Henriksen et al., 2012; Ibinson et al., 2022; Jiang et al., 2010; Tanaka et al., 2018) and suggests that PASL could reliably (with a good to excellent reliability) measure rs-CBF at the whole brain level. In contrast, the reliability of rs-CBF in single ROIs is highly variable: while some (such as the cerebellum or the occipital lobe) stay highly reliable over time, others drop drastically even by approaching ICC = 0 (such as the frontal or temporal lobe). Some ROIs were also more reliable when contrasting baseline to 8 weeks in comparison to 3 weeks interscan interval (such as the pallidum or the thalamus). This unexpected variability in reliability may suggest that those regions share more physiological day-to-day variability. For example, even at rest, specific brain areas can be affected by cognitive or emotional state (Claassen et al., 2021). This should hold particularly true for regions of the default mode network (Orosz et al., 2012).

At the clinical level, ASL has been used to describe disease-specific CBF alterations in various disorders, such as schizophrenia, depression, obsessive-compulsive disorder, or attention deficit hyperactivity disorder (Allen et al., 2016; Batail et al., 2023; Gangl et al., 2023; Legind et al., 2019; Nenadic et al., 2023; Oliver et al., 2023; Ota et al., 2020; Scheef et al., 2010; Stegmayer et al., 2017a, 2017b; Tang et al., 2023). Furthermore, ASL protocols were used to examine longitudinal changes in brain perfusion following interventions including transcranial magnetic stimulation, electroconvulsive therapy, and psychotropic medication (Alsop et al., 2015; Bracht et al., 2023; Klomp et al., 2012; Zhu et al., 2017). In addition, researchers explored brain-behavior associations using ASL. For example, resting-state CBF (rs-CBF) changes were linked with the severity of catatonia, as the supplementary motor area was found to be hyperperfused, while activity level correlated to the perfusion rate of cortical motor areas in patients with psychomotor slowing in depression and psychosis (Cantisani et al., 2016; Walther et al., 2011, 2012, 2017). The increasing use of tracer-free brain perfusion measurements such as ASL highlights its importance in detecting pathological changes in neuropsychiatric disorders. In this regard, our data suggests that the motor circuit has good reliability over three weeks, which is important for monitoring interventions such as repetitive transcranial magnetic stimulation (Lefebvre et al., 2020; Walther et al.,

2020a, 2024, 2017) or for understanding pathobiology of the motor system (Lefebvre et al., 2024; Moussa-Tooks et al., 2024). Furthermore, areas of the so-called praxis network seem to also have good reliability, which is important when studying interventions for patients with schizophrenia, stroke or Parkinson's disease (Kubel et al., 2018; Pastore-Wapp et al., 2022; Viher et al., 2020; Walther et al., 2020b). Finally, also limbic areas seem to have good reliability over 3 and 8 weeks, which is important when studying neural correlates of paranoia (Kindler et al., 2015; Pinkham et al., 2015; Stegmayer et al., 2017c; Walther et al., 2022). Accordingly, the present results suggest that rs-CBF reliability could be used to explore the neural substrate underlying longitudinal changes or response to interventions in clinical populations, particularly in psychiatric disorders.

The present study suffered from several limitations. First, the sample sizes of the two analyzed datasets were relatively small. However, the initial sample sizes were adequate to the sample size estimation for hypothesis-driven ICC calculation. Unfortunately, the analyzed datasets were reduced due to quality control-based exclusion. Furthermore, it remains unclear whether reliability estimates in healthy controls may generalize to patients with neuropsychiatric disorders, as brain pathology and illness-related life-style changes such as smoking may affect local rs-CBF values. Despite these considerations, the present study is still the largest one, up to now, to evaluate rs-CBF reliability in healthy participants. Moreover, the interscan periods were limited to 3 and 8 weeks. Then, the evaluation of the reliability over the two different interscan periods was performed in two different sets of participants. Even if the baseline rs-CBF measurements were similar between them, difference in reliability between 3 and 8 weeks might be due to inner difference between the two samples. Future studies including more participants assessed multiple times over longer periods would help to provide a better understanding of the reliability of the rs-CBF assessment. In this study, we lack information on whether individuals kept their eyes open or closed during the acquisition of wakeful resting-state MRI. Subjects received no specific instruction besides to stay awake. With eyes open participants are more likely to process incoming visual information, whereas during eyes closed mind wandering is more likely. Studies on resting-state either instruct participants to open or to close their eyes. Therefore, the resting-state of this study includes some interindividual variance that may have contributed to signal fluctuations. Finally, this study used PASL to quantify rs-CBF, compared to other available sequences, PASL has a shorter radiofrequency pulse, and therefore a smaller labeled bolus which leads to a lower signal-to-noise ratio that may negatively affect image resolution. Nevertheless, PASL is often used in clinical settings because it is easier to implement (Alsop et al., 2015).

To conclude, in line with previous studies, we demonstrated, that ASL provides an overall reliable rs-CBF estimation which may serve as

Table 4

ICC per ROIs for the two samples

This table displays the reliability of the rs-CBF for each ROI of the atlas for the two samples. ICC are classified according to the following color code: poor <0.4: red; fair 0.4–0.6: yellow; good 0.6–0.75: green; excellent >0.75: dark green. The table also displays the power calculation for each obtained ICC.

ICC: intraclass correlation coefficient; Sample-3W: sample for the 3-week interscan interval; Sample-8W: sample for the 8-week interscan interval; CI:confidence interval; ROI: Region of interest; rs-CBF: resting-state cerebral blood flow; ant.: anterior; inf.:inferior; post.: posterior; BL bilateral, L left, R right.

Part A per tissue type

Group	Average ICC (CI 95%, lower bound- upper bound)				
	Whole Brain	Right white matter	Left white matter	Right grey matter	Left grey matter
Sample-3W	0.847 (0.670-0.929)	0.824 (0.62-0.919)	0.802 (0.572-0.908)	0.83 (0.632-0.921)	0.803 (0.575-0.909)
Power	*0.82*	*0.70*	*0.57*	*0.73*	*0.58*
Sample-8W	0.529 (-0.22-0.82)	0.562 (-0.136-0.831)	0.388 (-0.589-0.764)	0.453 (-0.42-0.789)	0.254 (-0.937-0.712)
Power	*0.10*	*0.14*	*0.02*	*0.05*	*0.01*

Part B : ROIs of the Harvard-Oxford parcellation for bilateral, left, and right hemispheres

	Angular Gyrus			Ant. Cingulate Gyrus			Ant.Inferior Temporal Gyrus			Ant. Middle Temporal Gyrus			Ant. Parahippocampal Gyrus			Ant. Superior Temporal Gyrus			Ant Supramarginal Gyrus			Ant.Temporal Fusiform Cortex			Brain-Stem			Central Opercular Cortex			Cerebellum		
	BL	L	R	BL	L	R	BL	L	R	BL	L	R	BL	L	R	BL	L	R	BL	L	R	BL	L	R	BL	L	R	BL	L	R	BL	L	R
Sample-3W	.681	.798	.689	.764	.465	.821	.695	.738	.589	.753	.735	.727	.632	.675	.605	.585	.673	.537	.659	.703	.613	.594	.626	.460	.666	.450	.439	.764	.787	.691	.85	.822	.842
Power	.107	.547	.122	.369	.002	.679	.134	.259	.020	.319	.248	.221	.045	.097	.027	.019	.093	.007	.073	.153	.032	.022	.041	.001	.083	.001	.001	.369	.486	.126	.833	.685	.794
Sample-8W	.286	0	.464	.457	.270	.444	.337	.514	0	.02	.315	0	.623	.710	.411	0	.022	.290	.368	.497	.069	.73	.652	.668	.474	.275	.502	.761	.742	.778
Power	<.001	<.001	.003	.003	<.001	.002	<.001	.006	<.001	<.001	<.001	<.001	.036	.128	.001	<.001	<.001	<.001	.001	.005	<.001	.168	.055	.070	.003	<.001	.005	.253	.198	.313

	Cuneal Cortex			Frontal Medial Cortex			Frontal Operculum Cortex			Frontal Orbital Cortex			Frontal Pole			Heschl's Gyrus			Inf. Lateral Occipital Cortex			Insular Cortex			Intracalcarine Cortex			Juxtapositional Lobule Cortex			Accumbens		
	BL	L	R	BL	L	R	BL	L	R	BL	L	R	BL	L	R	BL	L	R	BL	L	R	BL	L	R	BL	L	R	BL	L	R	BL	L	R
Sample-3W	.75	.791	.764	.726	.522	.823	.671	.624	.646	.531	.528	.534	.614	.596	.698	.688	.817	.632	.677	.704	.750	.623	.770	.548	.749	.761	.718	.597	.537	.714	.278	.386	.495
Power	.306	.508	.369	.218	.005	.691	.090	.039	.058	.006	.006	.007	.033	.023	.141	.120	.656	.045	.100	.155	.306	.038	.397	.009	.302	.355	.193	.024	.007	.182	<.001	<.001	.003
Sample-8W	.503	.386	.466	0	0	0	.54	.419	.515	.285	.290	.385	0	0	0	.116	.073	.203	.307	.294	.313	.496	.412	.498	.575	.493	.431	0	0	0	.418	.56	.401
Power	.005	.001	.003	<.001	<.001	<.001	.010	.001	.006	<.001	<.001	.001	<.001	<.001	<.001	<.001	<.001	<.001	.005	.001	.005	.017	.005	.002	<.001	<.001	<.001	.001	.013	.001

	Amygdala			Caudate			Hippocampus			Lateral Ventricle			Pallidum			Putamen			Thalamus			Lingual Gyrus			Middle Frontal Gyrus			Occipital Fusiform Gyrus			Occipital Pole		
	BL	L	R	BL	L	R	BL	L	R	BL	L	R	BL	L	R	BL	L	R	BL	L	R	BL	L	R	BL	L	R	BL	L	R	BL	L	R
Sample-3W	.486	.616	.379	.243	.407	.338	.340	.426	.549	.087	0	.215	.301	.269	.178	.512	.636	.475	.253	.348	.302	.667	.707	.717	.793	.747	.765	.629	.714	.681	.743	.773	.796
Power	.003	.034	<.001	<.001	<.001	<.001	<.001	.001	.009	<.001	<.001	<.001	<.001	<.001	<.001	.004	.049	.002	<.001	<.001	<.001	.084	.163	.190	.519	.294	.373	.043	.182	.107	.278	.412	.536
Sample-8W	.606	.616	.532	.649	.688	.796	.651	.713	.787	.652	.703	.787	.778	.752	.841	.723	.728	.799	.784	.788	.813	.713	.628	.563	.092	0	.199	.655	.582	.571	.623	.676	.636
Power	.027	.032	.009	.053	.094	.387	.054	.133	.349	.055	.116	.349	.313	.226	.616	.153	.164	.401	.337	.353	.467	.133	.038	.014	<.001	<.001	<.001	.058	.019	.016	.036	.079	.043

	Paracingulate Gyrus			Parietal Operculum Cortex			ParsO.Inferior Frontal Gyrus			ParsT. Inferior Frontal Gyrus			Planum Polare			Planum Temporale			Post.Cingulate Gyrus			Post.Inferior Temporal Gyrus			Post.Middle Temporal Gyrus			Post.Parahippocampal Gyrus			Post.Superior Temporal Gyrus		
	BL	L	R	BL	L	R	BL	L	R	BL	L	R	BL	L	R	BL	L	R	BL	L	R	BL	L	R	BL	L	R	BL	L	R	BL	L	R
Sample-3W	.795	.500	.843	.816	.863	.716	.760	.722	.752	.776	.743	.726	.552	.694	.454	.822	.860	.778	.512	.391	.615	.717	.785	.562	.795	.760	.747	.543	.543	.651	.815	.830	.810
Power	.530	.003	.799	.650	.889	.187	.486	.205	.315	.428	.278	.218	.010	.132	.001	.685	.877	.438	.004	<.001	.033	.190	.475	.012	.530	.350	.294	.008	.008	.064	.645	.730	.616
Sample-8W	.036	.127	0	.397	.232	.426	.72	.677	.670	.706	.633	.663	.024	0	.140	.28	.195	.310	.607	.323	.431	0	.130	0	.008	.117	0	.752	.697	.564	.104	.147	.080
Power	<.001	<.001	<.001	.001	<.001	.001	.147	.080	.072	.121	.041	.065	<.001	<.001	<.001	<.001	<.001	<.001	.028	<.001	.002	<.001	<.001	<.001	<.001	<.001	<.001	.226	.106	.014	<.001	<.001	<.001

	Post. Supramarginal Gyrus			Post. Temporal Fusiform Cortex			Postcentral Gyrus			Precentral Gyrus			Precuneous Cortex			Subcallosal Cortex			Sup.Lateral Occipital Cortex			Superior Frontal Gyrus			Superior Parietal Lobule			Supracalcarine Cortex			Temporal Pole		
	BL	L	R	BL	L	R	BL	L	R	BL	L	R	BL	L	R	BL	L	R	BL	L	R	BL	L	R	BL	L	R	BL	L	R	BL	L	R
Sample-3W	.758	.833	.715	.748	.816	.701	.605	.662	.648	.719	.720	.734	.611	.591	.705	.388	.389	.573	.641	.722	.758	.747	.657	.703	.492	.658	.541	.729	.740	.753	.613	.594	.503
Power	.341	.746	.184	.298	.650	.148	.027	.077	.060	.196	.199	.245	.031	.021	.158	<.001	<.001	.015	.053	.205	.341	.294	.071	.153	.003	.072	.008	.228	.267	.319	.032	.022	.004
Sample-8W	.247	.045	.365	.315	.540	0	0	0	0	0	0	0	.248	.119	.335	.058	.066	.048	.274	.115	.456	0	0	0	0	0	0	.444	.262	.362	.684	.713	.590
Power	<.001	<.001	.001	<.001	.010	<.001	<.001	<.001	<.001	<.001	<.001	<.001	<.001	<.001	<.001	<.001	<.001	.002	<.001	<.001	<.001	<.001	<.001	<.001	<.001	<.001	<.001	.002	<.001	<.001	.088	.133	.021

biomarker for resting neural activity in neurological and psychiatric diseases. As the reliability of the rs-CBF quantification seemed to decrease after several weeks, caution is warranted when performing correlations with other variables, especially in clinical populations.

CRediT authorship contribution statement

Alexandra Kyrou: Writing – review & editing, Writing – original draft, Visualization, Investigation, Formal analysis, Data curation. **Elina Grünert:** Writing – review & editing, Writing – original draft, Visualization, Methodology, Investigation, Formal analysis, Data curation. **Florian Wüthrich:** Writing – review & editing, Writing – original draft, Methodology, Funding acquisition, Formal analysis, Conceptualization. **Niluja Nadesalingam:** Writing – review & editing, Validation, Data
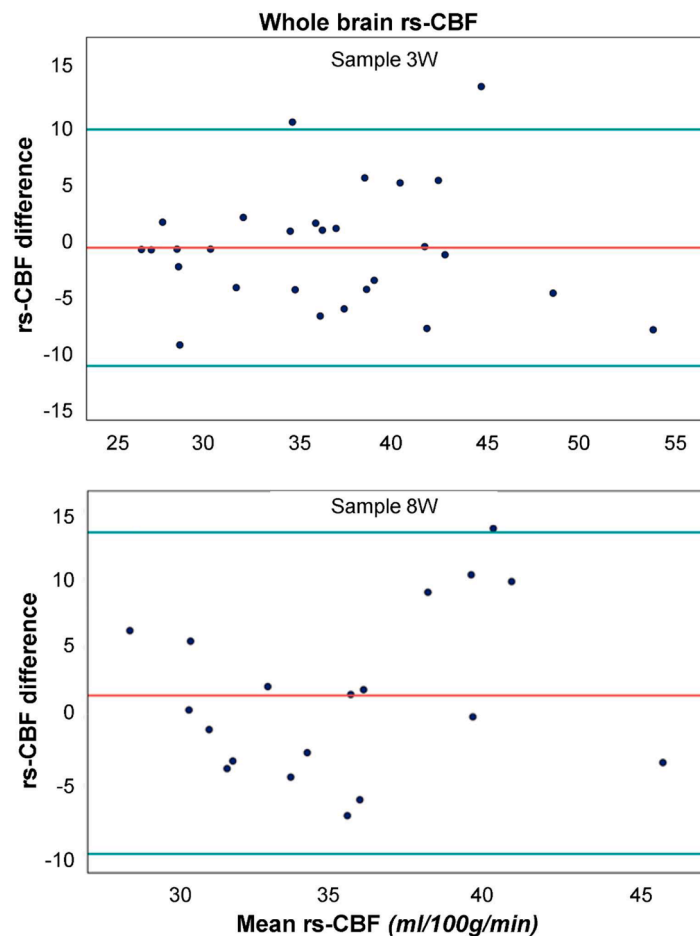
Fig. 3. Bland Altman Plots of the rs-CBF values for the whole brain.
Bland Altman plots are a graphic method to analyze the agreement between two different sessions. The red line represents the mean difference between the two measurements, whereas the green lines represent the 95 % confidence interval (mean±1.96 *SD*). Values approaching the mean difference line represent better reliability.
Sample-3W: sample for the 3-week interscan interval; Sample-8W: sample for the 8-week interscan interval; p value. ICC: intraclass correlation coefficient; rs-CBF: resting-state cerebral blood flow. (For interpretation of the references to colour in this figure legend, the reader is referred to the web version of this article.)

curation. **Victoria Chapellier:** Writing – review & editing, Validation, Data curation. **Melanie G Nuoffer:** Writing – review & editing, Validation, Data curation. **Anastasia Pavlidou:** Writing – review & editing, Validation, Supervision, Methodology. **Stephanie Lefebvre:** Writing – review & editing, Writing – original draft, Visualization, Validation, Supervision, Project administration, Methodology, Investigation, Formal analysis, Conceptualization. **Sebastian Walther:** Writing – review & editing, Writing – original draft, Validation, Supervision, Investigation, Funding acquisition, Conceptualization.

Declaration of competing interest

References

Allen, P., Chaddock, C.A., Egerton, A., Howes, O.D., Bonoldi, I., Zelaya, F., Bhattacharyya, S., Murray, R., McGuire, P., 2016. Resting Hyperperfusion of the Hippocampus, Midbrain, and Basal Ganglia in People at High Risk for Psychosis. Am. J. Psychiatry 173 (4), 392–399.
Almeida, J.R.C., Greenberg, T., Lu, H., Chase, H.W., Fournier, J.C., Cooper, C.M., Deckersbach, T., Adams, P., Carmody, T., Fava, M., Kurian, B., McGrath, P.J., McInnis, M.G., Oquendo, M.A., Parsey, R., Weissman, M., Trivedi, M., Phillips, M.L., 2018. Test-retest reliability of cerebral blood flow in healthy individuals using arterial spin labeling: findings from the EMBARC study. Magn. Reson. ImAging 45, 26–33.
Alsaedi, A., Thomas, D., Bisdas, S., Golay, X., 2018. Overview and Critical Appraisal of Arterial Spin Labelling Technique in Brain Perfusion Imaging. Contrast. Media Mol. ImAging 2018, 5360375.
Alsop, D.C., Detre, J.A., Golay, X., Gunther, M., Hendrikse, J., Hernandez-Garcia, L., Lu, H., MacIntosh, B.J., Parkes, L.M., Smits, M., van Osch, M.J., Wang, D.J., Wong, E. C., Zaharchuk, G., 2015. Recommended implementation of arterial spin-labeled perfusion MRI for clinical applications: a consensus of the ISMRM perfusion study group and the European consortium for ASL in dementia. Magn. Reson. Med. 73 (1), 102–116.
Batail, J.M., Corouge, I., Combes, B., Conan, C., Guillery-Sollier, M., Verin, M., Sauleau, P., Le Jeune, F., Gauvrit, J.Y., Robert, G., Barillot, C., Ferre, J.C., Drapier, D., 2023. Apathy in depression: an arterial spin labeling perfusion MRI study. J. Psychiatr. Res. 157, 7–16.
Bland, J.M., Altman, D.G., 1996. Measurement error proportional to the mean. BMJ 313 (7049), 106.
Borogovac, A., Asllani, I., 2012. Arterial Spin Labeling (ASL) fMRI: advantages, theoretical constrains, and experimental challenges in neurosciences. Int. J. Biomed. ImAging 2012, 818456.
Bracht, T., Walther, S., Breit, S., Mertse, N., Federspiel, A., Meyer, A., Soravia, L.M., Wiest, R., Denier, N., 2023. Distinct and shared patterns of brain plasticity during electroconvulsive therapy and treatment as usual in depression: an observational multimodal MRI-study. Transl. Psychiatry 13 (1), 6.

Buxton, R.B., Frank, L.R., 1997. A model for the coupling between cerebral blood flow and oxygen metabolism during neural stimulation. J. Cereb. Blood Flow Metab. 17 (1), 64–72.

Cantisani, A., Stegmayer, K., Bracht, T., Federspiel, A., Wiest, R., Horn, H., Muller, T.J., Schneider, C., Hofle, O., Strik, W., Walther, S., 2016. Distinct resting-state perfusion patterns underlie psychomotor retardation in unipolar vs. bipolar depression. Acta Psychiatr. Scand. 134 (4), 329–338.

Chapellier, V., Pavlidou, A., Mueller, D.R., Walther, S., 2022. Brain Stimulation and Group Therapy to Improve Gesture and Social Skills in Schizophrenia-The Study Protocol of a Randomized, Sham-Controlled, Three-Arm, Double-Blind Trial. Front. Psychiatry 13, 909703.

Chen, Y., Wang, D.J., Detre, J.A., 2011. Test-retest reliability of arterial spin labeling with common labeling strategies. J. Magn. Reson. Imaging 33 (4), 940–949.

Cicchetti, D.V., 1994. Guidelines, criteria, and rules of thumb for evaluating normed and standardized assessment instruments in psychology. Psychol. Assess. 6, 284–290.

Claassen, J., Thijssen, D.H.J., Panerai, R.B., Faraci, F.M., 2021. Regulation of cerebral blood flow in humans: physiology and clinical implications of autoregulation. Physiol. Rev. 101 (4), 1487–1559.

Desikan, R.S., Segonne, F., Fischl, B., Quinn, B.T., Dickerson, B.C., Blacker, D., Buckner, R.L., Dale, A.M., Maguire, R.P., Hyman, B.T., Albert, M.S., Killiany, R.J., 2006. An automated labeling system for subdividing the human cerebral cortex on MRI scans into gyral based regions of interest. Neuroimage 31 (3), 968–980.

Endicott, J., Spitzer, R.L., Fleiss, J.L., Cohen, J., 1976. The global assessment scale. A procedure for measuring overall severity of psychiatric disturbance. Arch. Gen. Psychiatry 33 (6), 766–771.

Fallatah, S.M., Pizzini, F.B., Gomez-Anson, B., Magerkurth, J., De Vita, E., Bisdas, S., Jager, H.R., Mutsaerts, H., Golay, X., 2018. A visual quality control scale for clinical arterial spin labeling images. Eur. Radiol. Exp. 2 (1), 45.

Frazier, J.A., Chiu, S., Breeze, J.L., Makris, N., Lange, N., Kennedy, D.N., Herbert, M.R., Bent, E.K., Koneru, V.K., Dieterich, M.E., Hodge, S.M., Rauch, S.L., Grant, P.E., Cohen, B.M., Seidman, L.J., Caviness, V.S., Biederman, J., 2005. Structural brain magnetic resonance imaging of limbic and thalamic volumes in pediatric bipolar disorder. Am. J. Psychiatry 162 (7), 1256–1265.

Gangl, N., Conring, F., Federspiel, A., Wiest, R., Walther, S., Stegmayer, K., 2023. Resting-state perfusion in motor and fronto-limbic areas is linked to diminished expression of emotion and speech in schizophrenia. Schizophrenia (Heidelb) 9 (1), 51.

Gevers, S., van Osch, M.J., Bokkers, R.P., Kies, D.A., Teeuwisse, W.M., Majoie, C.B., Hendrikse, J., Nederveen, A.J., 2011. Intra- and multicenter reproducibility of pulsed, continuous and pseudo-continuous arterial spin labeling methods for measuring cerebral perfusion. J. Cereb. Blood Flow Metab. 31 (8), 1706–1715.

Giraudeau, B., Ravaud, P., Chastang, C., 2000. Comment on Quan and Shih's "Assessing reproducibility by the within-subject coefficient of variation with random effects models". Biometrics 56 (1), 301–302.

Golay, X., Hendrikse, J., Lim, T.C., 2004. Perfusion imaging using arterial spin labeling. Top. Magn. Reson. Imaging 15 (1), 10–27.

Goldstein, J.M., Seidman, L.J., Makris, N., Ahern, T., O'Brien, L.M., Caviness Jr, V.S., Kennedy, D.N., Faraone, S.V., Tsuang, M.T., 2007. Hypothalamic abnormalities in schizophrenia: sex effects and genetic vulnerability. Biol. Psychiatry 61 (8), 935–945.

Grade, M., Hernandez Tamames, J.A., Pizzini, F.B., Achten, E., Golay, X., Smits, M., 2015. A neuroradiologist's guide to arterial spin labeling MRI in clinical practice. Neuroradiology 57 (12), 1181–1202.

Haller, S., Zaharchuk, G., Thomas, D.L., Lovblad, K.O., Barkhof, F., Golay, X., 2016. Arterial Spin Labeling Perfusion of the Brain: emerging Clinical Applications. Radiology 281 (2), 337–356.

Henriksen, O.M., Larsson, H.B., Hansen, A.E., Gruner, J.M., Law, I., Rostrup, E., 2012. Estimation of intersubject variability of cerebral blood flow measurements using MRI and positron emission tomography. J. Magn. Reson. Imaging 35 (6), 1290–1299.

Hernandez-Garcia, L., Lahiri, A., Schollenberger, J., 2019. Recent progress in ASL. Neuroimage 187, 3–16.

Ho, M.L., 2018. Arterial spin labeling: clinical applications. J. Neuroradiol. 45 (5), 276–289.

Ibinson, J.W., Gillman, A.G., Schmidthorst, V., Li, C., Napadow, V., Loggia, M.L., Wasan, A.D., 2022. Comparison of test-retest reliability of BOLD and pCASL fMRI in a two-center study. BMC. Med. ImAging 22 (1), 62.

Jiang, L., Kim, M., Chodkowski, B., Donahue, M.J., Pekar, J.J., Van Zijl, P.C., Albert, M., 2010. Reliability and reproducibility of perfusion MRI in cognitively normal subjects. Magn. Reson. ImAging 28 (9), 1283–1289.

Kindler, J., Jann, K., Homan, P., Hauf, M., Walther, S., Strik, W., Dierks, T., Hubl, D., 2015. Static and dynamic characteristics of cerebral blood flow during the resting state in schizophrenia. Schizophr. Bull. 41 (1), 163–170.

Klomp, A., Caan, M.W., Denys, D., Nederveen, A.J., Reneman, L., 2012. Feasibility of ASL-based phMRI with a single dose of oral citalopram for repeated assessment of serotonin function. Neuroimage 63 (3), 1695–1700.

Koo, T.K., Li, M.Y., 2016. A Guideline of Selecting and Reporting Intraclass Correlation Coefficients for Reliability Research. J. Chiropr. Med. 15 (2), 155–163.

Kubel, S., Stegmayer, K., Vanbellingen, T., Walther, S., Bohlhalter, S., 2018. Deficient supplementary motor area at rest: neural basis of limb kinetic deficits in Parkinson's disease. Hum. Brain Mapp. 39 (9), 3691–3700.

Lefebvre, S., Gehrig, G., Nadesalingam, N., Nuoffer, M.G., Kyrou, A., Wuthrich, F., Walther, S., 2024. The pathobiology of psychomotor slowing in psychosis: altered cortical excitability and connectivity. Brain 147 (4), 1423–1435.

Lefebvre, S., Pavlidou, A., Walther, S., 2020. What is the potential of neurostimulation in the treatment of motor symptoms in schizophrenia? Expert. Rev. NeurOther 20 (7), 697–706.

Legind, C.S., Broberg, B.V., Brouwer, R., Mandl, R.C.W., Ebdrup, B.H., Anhoj, S.J., Jensen, M.H., Hilker, R., Fagerlund, B., Hulshoff Pol, H.E., Glenthoj, B.Y., Rostrup, E., 2019. Heritability of Cerebral Blood Flow and the Correlation to Schizophrenia Spectrum Disorders: a Pseudo-continuous Arterial Spin Labeling Twin Study. Schizophr. Bull. 45 (6), 1231–1241.

Maderthaner, L., Pavlidou, A., Lefebvre, S., Nadesalingam, N., Chapellier, V., von Kanel, S., Kyrou, A., Alexaki, D., Wuthrich, F., Weiss, F., Baumann-Gama, D., Wiest, R., Strik, W., Kircher, T., Walther, S., 2023. Neural Correlates of Formal Thought Disorder Dimensions in Psychosis. Schizophr. Bull. 49 (Suppl_2), S104–S114.

Makris, N., Goldstein, J.M., Kennedy, D., Hodge, S.M., Caviness, V.S., Faraone, S.V., Tsuang, M.T., Seidman, L.J., 2006. Decreased volume of left and total anterior insular lobule in schizophrenia. Schizophr. Res. 83 (2–3), 155–171.

Mezue, M., Segerdahl, A.R., Okell, T.W., Chappell, M.A., Kelly, M.E., Tracey, I., 2014. Optimization and reliability of multiple postlabeling delay pseudo-continuous arterial spin labeling during rest and stimulus-induced functional task activation. J. Cereb. Blood Flow Metab. 34 (12), 1919–1927.

Moussa-Tooks, A.B., Beermann, A., Felix, K.M., Coleman, M., Bouix, S., Holt, D., Lewandowski, K.E., Ongur, D., Breier, A., Shenton, M.E., Heckers, S., Walther, S., Brady, R.O., Jr., Ward, H.B., 2024. Isolation of Distinct Networks Driving Action and Cognition in Psychomotor Processes. Biol Psychiatry.

Muller, M., Wuthrich, F., Federspiel, A., Wiest, R., Egloff, N., Reichenbach, S., Exadaktylos, A., Juni, P., Curatolo, M., Walther, S., 2021. Altered central pain processing in fibromyalgia-A multimodal neuroimaging case-control study using arterial spin labelling. PLoS. One 16 (2), e0235879.

Nenadic, I., Meller, T., Evermann, U., Pfarr, J.K., Federspiel, A., Walther, S., Grezellschak, S., Abu-Akel, A., 2023. Modelling the overlap and divergence of autistic and schizotypal traits on hippocampal subfield volumes and regional cerebral blood flow. Mol. Psychiatry.

Oldfield, R.C., 1971. The assessment and analysis of handedness: the Edinburgh inventory. Neuropsychologia 9 (1), 97–113.

Oliver, D., Davies, C., Zelaya, F., Selvaggi, P., De Micheli, A., Catalan, A., Baldwin, H., Arribas, M., Modinos, G., Crossley, N.A., Allen, P., Egerton, A., Jauhar, S., Howes, O.D., McGuire, P., Fusar-Poli, P., 2023. Parsing neurobiological heterogeneity of the clinical high-risk state for psychosis: a pseudo-continuous arterial spin labelling study. Front. Psychiatry 14, 1092213.

Orosz, A., Jann, K., Federspiel, A., Horn, H., Hofle, O., Dierks, T., Wiest, R., Strik, W., Muller, T., Walther, S., 2012. Reduced cerebral blood flow within the default-mode network and within total gray matter in major depression. Brain Connect. 2 (6), 303–310.

Ota, M., Kanie, A., Kobayashi, Y., Nakajima, A., Sato, N., Horikoshi, M., 2020. Pseudo-continuous arterial spin labeling MRI study of patients with obsessive-compulsive disorder. Psychiatry Res. NeuroimAging 303, 111124.

Pastore-Wapp, M., Gyurko, D.M., Vanbellingen, T., Lehnick, D., Cazzoli, D., Pflugshaupt, T., Pflugi, S., Nyffeler, T., Walther, S., Bohlhalter, S., 2022. Improved gesturing in left-hemispheric stroke by right inferior parietal theta burst stimulation. Front. Neurosci. 16, 998729.

Pinkham, A.E., Liu, P., Lu, H., Kriegsman, M., Simpson, C., Tamminga, C., 2015. Amygdala Hyperactivity at Rest in Paranoid Individuals With Schizophrenia. Am. J. Psychiatry 172 (8), 784–792.

Scheef, L., Manka, C., Daamen, M., Kuhn, K.U., Maier, W., Schild, H.H., Jessen, F., 2010. Resting-state perfusion in nonmedicated schizophrenic patients: a continuous arterial spin-labeling 3.0-T MR study. Radiology 256 (1), 253–260.

Shrout, P.E., Fleiss, J.L., 1979. Intraclass correlations: uses in assessing rater reliability. Psychol. Bull. 86 (2), 420–428.

Ssali, T., Anazodo, U.C., Bureau, Y., MacIntosh, B.J., Gunther, M., St Lawrence, K., 2016. Mapping Long-Term Functional Changes in Cerebral Blood Flow by Arterial Spin Labeling. PLoS. One 11 (10), e0164112.

Stegmayer, K., Stettler, M., Strik, W., Federspiel, A., Wiest, R., Bohlhalter, S., Walther, S., 2017a. Resting state perfusion in the language network is linked to formal thought disorder and poor functional outcome in schizophrenia. Acta Psychiatr. Scand. 136 (5), 506–516.

Stegmayer, K., Strik, W., Federspiel, A., Wiest, R., Bohlhalter, S., Walther, S., 2017b. Specific cerebral perfusion patterns in three schizophrenia symptom dimensions. Schizophr. Res.

Stegmayer, K., Strik, W., Federspiel, A., Wiest, R., Bohlhalter, S., Walther, S., 2017c. Specific cerebral perfusion patterns in three schizophrenia symptom dimensions. Schizophr. Res. 190, 96–101.

Tanaka, Y., Inoue, Y., Abe, Y., Miyatake, H., Hata, H., 2018. Reliability of 3D arterial spin labeling MR perfusion measurements: the effects of imaging parameters, scanner model, and field strength. Clin. Imaging 52, 23–27.

Tang, S., Liu, X., Nie, L., Qian, F., Chen, W., He, L., 2023. Three-dimensional pseudocontinuous arterial spin labeling perfusion imaging shows cerebral blood flow perfusion decline in attention-deficit/hyperactivity disorder children. Front. Psychiatry 14, 1064647.

Viher, P.V., Abdulkadir, A., Savadijev, P., Stegmayer, K., Kubicki, M., Makris, N., Karmacharya, S., Federspiel, A., Bohlhalter, S., Vanbellingen, T., Muri, R., Wiest, R., Strik, W., Walther, S., 2020. Structural organization of the praxis network predicts gesture production: evidence from healthy subjects and patients with schizophrenia. Cortex 132, 322–333.

Walter, S.D., Eliasziw, M., Donner, A., 1998. Sample size and optimal designs for reliability studies. Stat. Med. 17 (1), 101–110.

Walther, S., Alexaki, D., Schoretsanitis, G., Weiss, F., Vladimirova, I., Stegmayer, K., Strik, W., Schäppi, L., 2020a. Inhibitory Repetitive Transcranial Magnetic Stimulation to Treat Psychomotor Slowing: a Transdiagnostic, Mechanism-Based Randomized Double-Blind Controlled Trial. Schizophr. Bull. Open. 1 (1).

Walther, S., Alexaki, D., Weiss, F., Baumann-Gama, D., Kyrou, A., Nuoffer, M.G., Wuthrich, F., Lefebvre, S., Nadesalingam, N., 2024. Psychomotor Slowing in Psychosis and Inhibitory Repetitive Transcranial Magnetic Stimulation: a Randomized Clinical Trial. JAMa Psychiatry.

Walther, S., Federspiel, A., Horn, H., Razavi, N., Wiest, R., Dierks, T., Strik, W., Muller, T. J., 2011. Resting state cerebral blood flow and objective motor activity reveal basal ganglia dysfunction in schizophrenia. Psychiatry Res. 192 (2), 117–124.

Walther, S., Hofle, O., Federspiel, A., Horn, H., Hugli, S., Wiest, R., Strik, W., Muller, T.J., 2012. Neural correlates of disbalanced motor control in major depression. J. Affect. Disord. 136 (1–2), 124–133.

Walther, S., Kunz, M., Muller, M., Zurcher, C., Vladimirova, I., Bachofner, H., Scherer, K. A., Nadesalingam, N., Stegmayer, K., Bohlhalter, S., Viher, P.V., 2020b. Single Session Transcranial Magnetic Stimulation Ameliorates Hand Gesture Deficits in Schizophrenia. Schizophr. Bull. 46 (2), 286–293.

Walther, S., Lefebvre, S., Conring, F., Gangl, N., Nadesalingam, N., Alexaki, D., Wuthrich, F., Ruter, M., Viher, P.V., Federspiel, A., Wiest, R., Stegmayer, K., 2022. Limbic links to paranoia: increased resting-state functional connectivity between amygdala, hippocampus and orbitofrontal cortex in schizophrenia patients with paranoia. Eur. Arch. Psychiatry Clin. Neurosci. 272 (6), 1021–1032.

Walther, S., Schappi, L., Federspiel, A., Bohlhalter, S., Wiest, R., Strik, W., Stegmayer, K., 2017. Resting-State Hyperperfusion of the Supplementary Motor Area in Catatonia. Schizophr. Bull. 43 (5), 972–981.

Zhu, J., Zhuo, C., Xu, L., Liu, F., Qin, W., Yu, C., 2017. Altered Coupling Between Resting-State Cerebral Blood Flow and Functional Connectivity in Schizophrenia. Schizophr. Bull. 43 (6), 1363–1374.